Supplementary information

A mechanical knock-out system uncovers that loss of titin tension triggers muscle disease

Roberto Silva-Rojas[a,*], Natalia Vicente[a], Manuel Gavilán-Herrera[a], Verónica Labrador-Cantarero[a], Jon Sicilia[a], Olga Giménez-Sáez[a], Andra C. Dumitru[a,b], Mateo I. Sánchez[c], Mara Gato-Vilaseca[a], Diana Velázquez-Carreras[a], Juan Antonio López[a,d], Jesús Vázquez[a,d], Elías Herrero-Galán[a], Miguel A. López-Unzu[a], Maria Rosaria Pricolo[a], Jorge Alegre-Cebollada[a,*]

This file includes:

- Supplementary Figures S1-S10

- Supplementary Tables S1-S2

Supplementary Figures

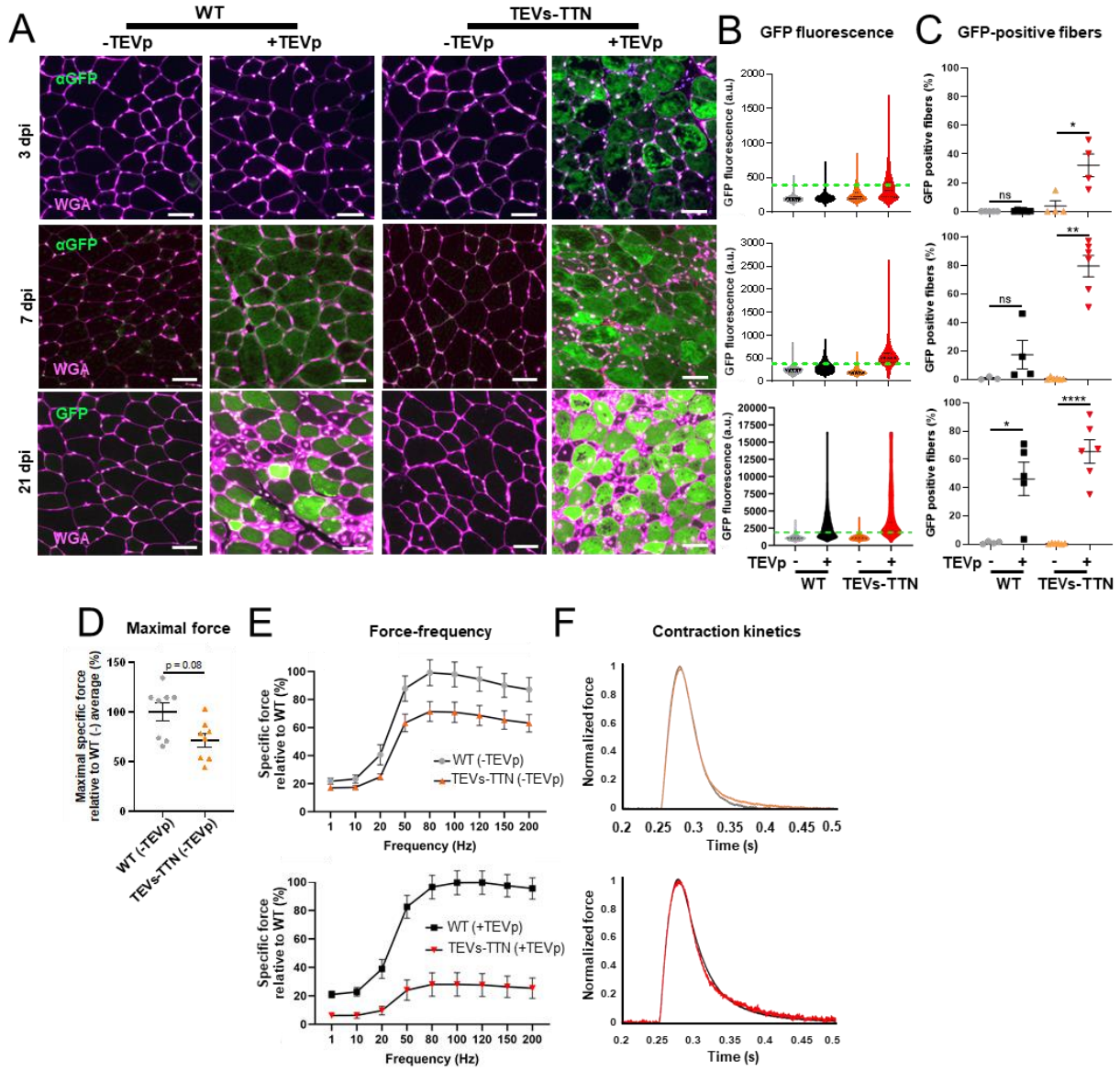

Figure S1. Phenotyping of titin mKO muscles. (A) GFP-TEVp immunofluorescence on transverse TA sections. Scale bars represent 50 µm. **(B, C)** Violin plot of GFP levels per individual myfiber. (B) and fraction of GFP-TEVp-positive myofibers (C) (n= 2949-9820 myofibers from 3-6 muscles per group, threshold marked with a dashed line). Experiments at different time points were done independently so the resulting GFP fluorescence intensities cannot be compared directly. **(D)** Maximal specific active force produced by control EDL muscles (n=7-8). Data are represented as mean ± SEM. **(E)** Specific force produced by EDL of the different groups at different stimulation frequencies at 7dpi. Data are represented as mean ± SEM. **(F)** Average normalized force kinetics upon single stimulation of muscles from the different groups (n=7-8).

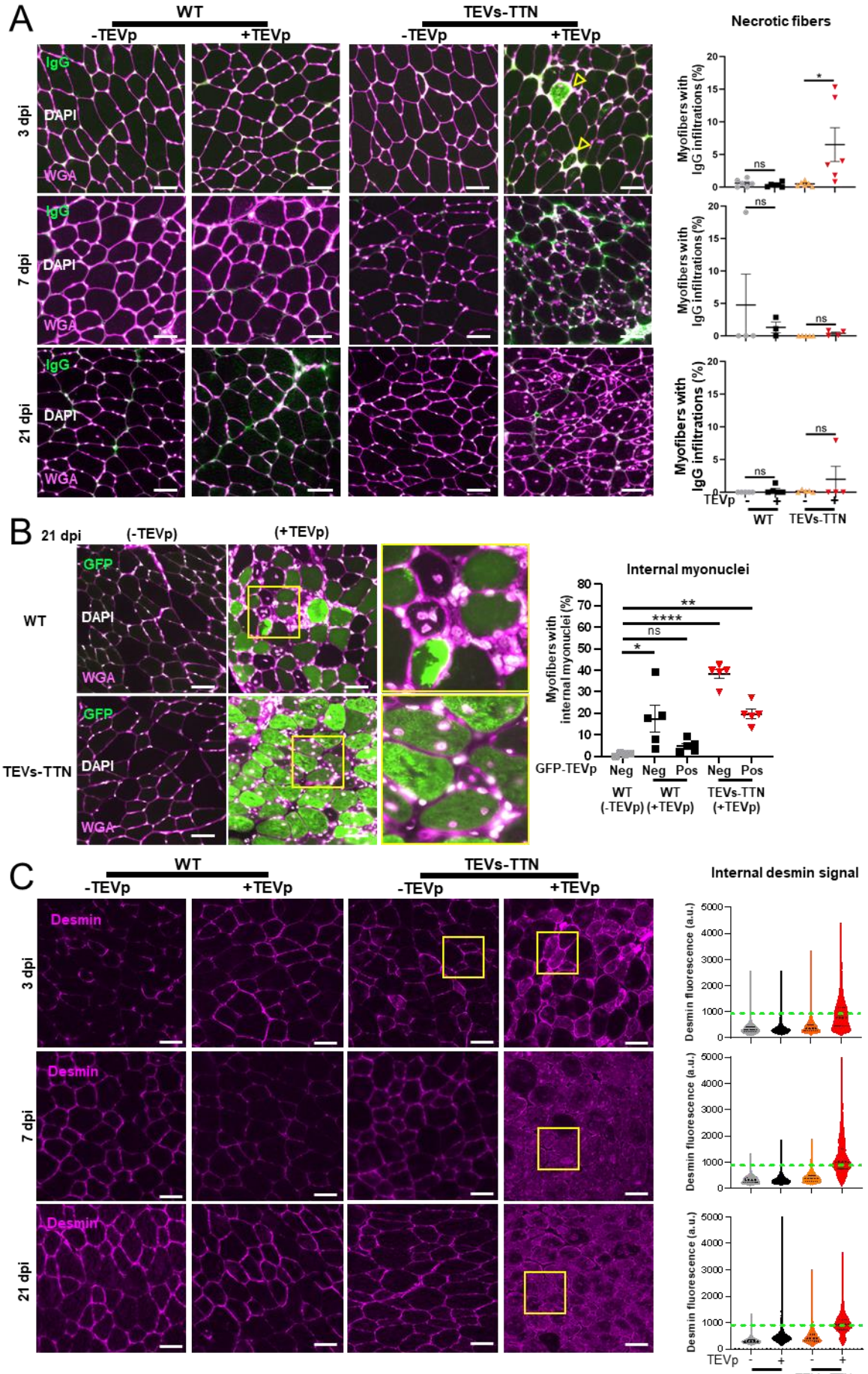
A
WT
TEVs-TTN
-TEVp
+TEVp
IgG
DAPI
WGA
3 dpi
7 dpi
21 dpi
Necrotic fibers
Myofibers with IgG infiltrations (%)
ns
*
TEVp
WT
TEVs-TTN
B
21 dpi
(-TEVp)
(+TEVp)
WT
TEVs-TTN
GFP
Internal myonuclei
Myofibers with internal myonuclei (%)
**
****
GFP-TEVp
Neg
Pos
WT (-TEVp)
WT (+TEVp)
TEVs-TTN (+TEVp)
C
Desmin
Internal desmin signal
Desmin fluorescence (a.u.)

Figure S2. Quantification of myofiber necrosis and myonuclei location. (A) Immunofluorescence using anti mouse IgG to study the presence of immunoglobulins in necrotic myofibers and quantification (n=3-6). Data are represented as mean ± SEM. Scale bars represent 50 µm. **(B)** GFP-TEVp immunofluorescence on transverse TA sections (regions zoomed on the left are indicated). Fraction of myofibers with internalized myonuclei depending on GFP-TEVp positivity. Data are represented as mean ± SEM. Scale bars represent 50 µm. **(C)** Desmin immunofluorescence in transverse TA sections and violin plots of its sarcoplasmic intensity in individual myofibers (n= 5293-11707 myofibers from 3-5 muscles per group). Boxes indicate highlighted regions in **Figure 2E**. The threshold used for quantification in **Figure 2F** is marked with a dashed line. Scale bars represent 50 µm.

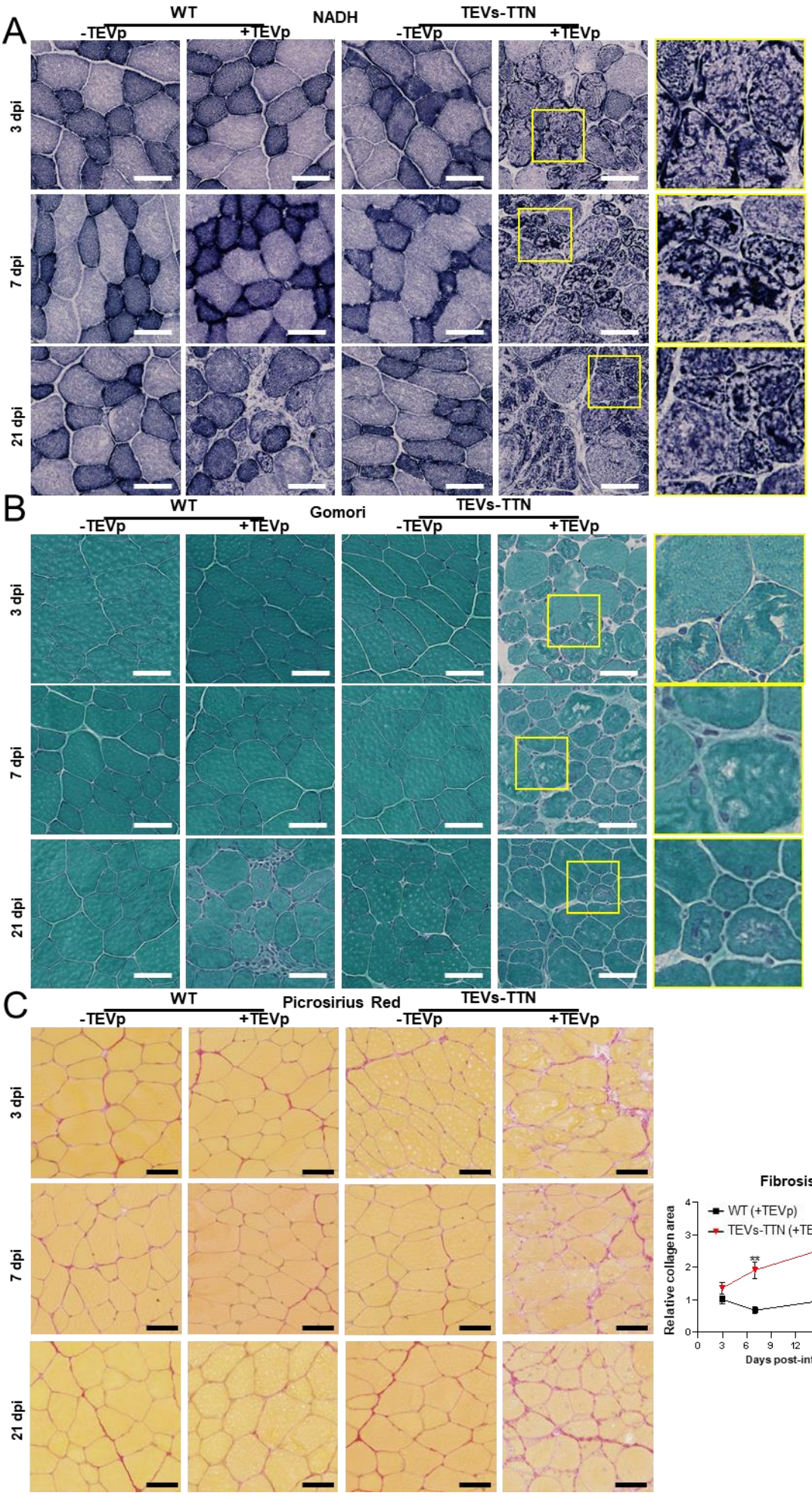
A
WT
NADH
TEVs-TTN
-TEVp
+TEVp
-TEVp
+TEVp
3 dpi
7 dpi
21 dpi
B
WT
Gomori
TEVs-TTN
-TEVp
+TEVp
-TEVp
+TEVp
3 dpi
7 dpi
21 dpi
C
WT
Picrosirius Red
TEVs-TTN
-TEVp
+TEVp
-TEVp
+TEVp
3 dpi
7 dpi
21 dpi
Fibrosis
WT (+TEVp)
TEVs-TTN (+TEVp)
Relative collagen area
Days post-infection
0
1
2
3
4
0
3
6
9
12
15
18
21
24
**
*

Figure S3. Mitochondrial mislocalization and aggregation and fibrosis induced by titin mKO. (A) NADH activity staining of muscle TA cryosections (n=5). Scale bars represent 50 µm. **(B)** Modified Gomori staining (n=5). Scale bars represent 50 µm. **(C)** Picrosirius staining marking mature collagen deposition and quantification of the fibrosis extent in AAV6-injected TA muscles normalized with their contralateral leg (n=5). Scale bars represent 50 µm. Data are represented as mean ± SEM.

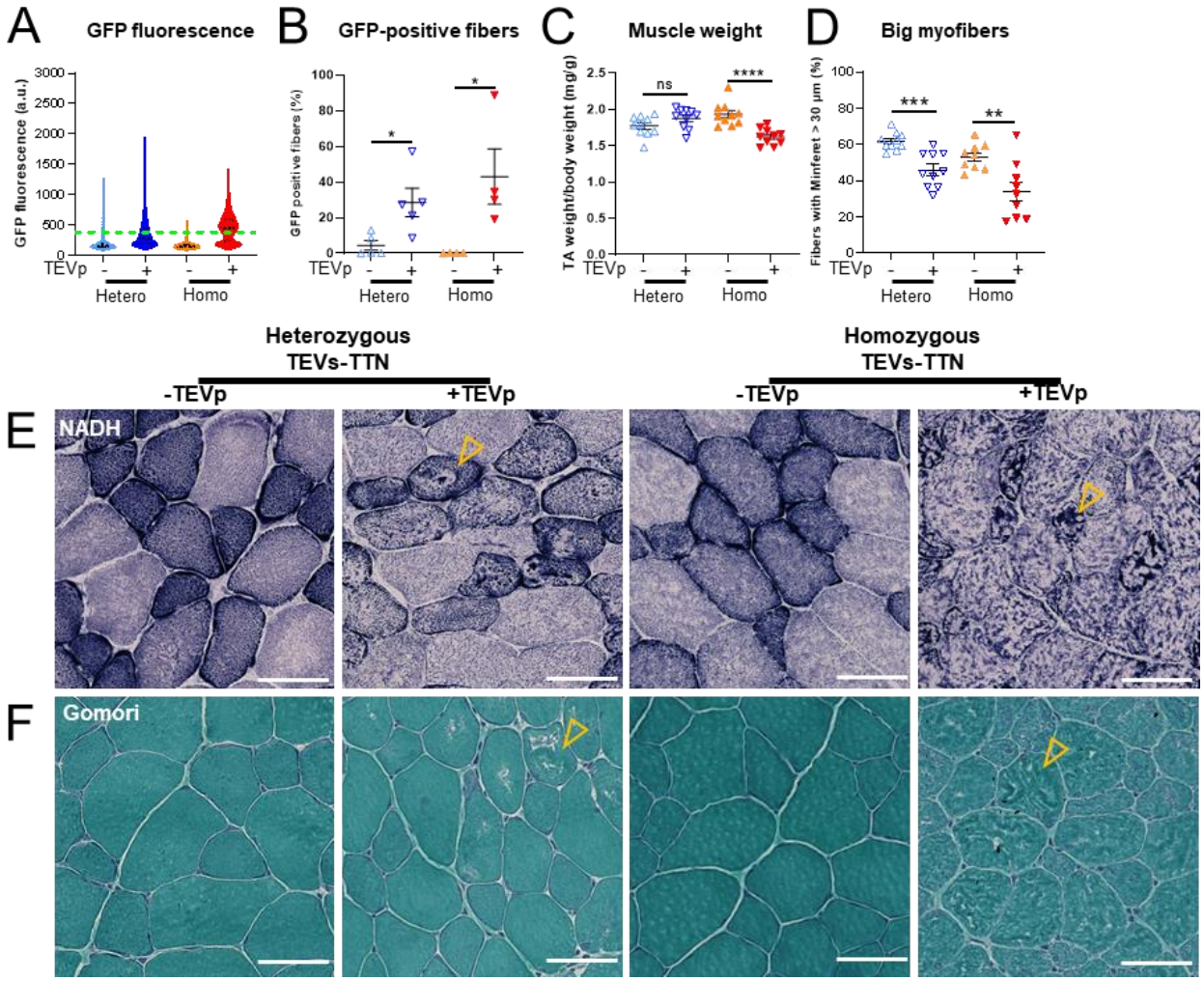

Figure S4. Comparative effects of GFP-TEVp expression in heterozygous and homozygous TEVs-TTN mice at 7 dpi. (A) Violin plot of GFP levels in the immunofluorescence shown in **Figure 3A** (n= 4834-7477 myofibers from 4-5 muscles per group, threshold marked with a dashed line). **(B)** Fraction of GFP-TEVp-positive myofibers (n=4-5). Data are represented as mean ± SEM. **(C)** TA muscle weight to body weight ratio (n=10). Data are represented as mean ± SEM. **(D)** Fraction of myofibers with MinFeret diameter larger than 30 µm (n=9-10). Data are represented as mean ± SEM. **(E)** NADH staining in heterozygous and homozygous mKO muscles. Arrowheads mark cores in heterozygous samples and mitochondrial mislocalization in homozygous samples (n=3-5). Scale bars represent 50 µm. **(F)** Gomori staining in heterozygous and homozygous mKO muscles. Arrowheads mark stain-free zones both in heterozygous and homozygous mKO muscles. (n=3-5). Scale bars represent 50 µm.

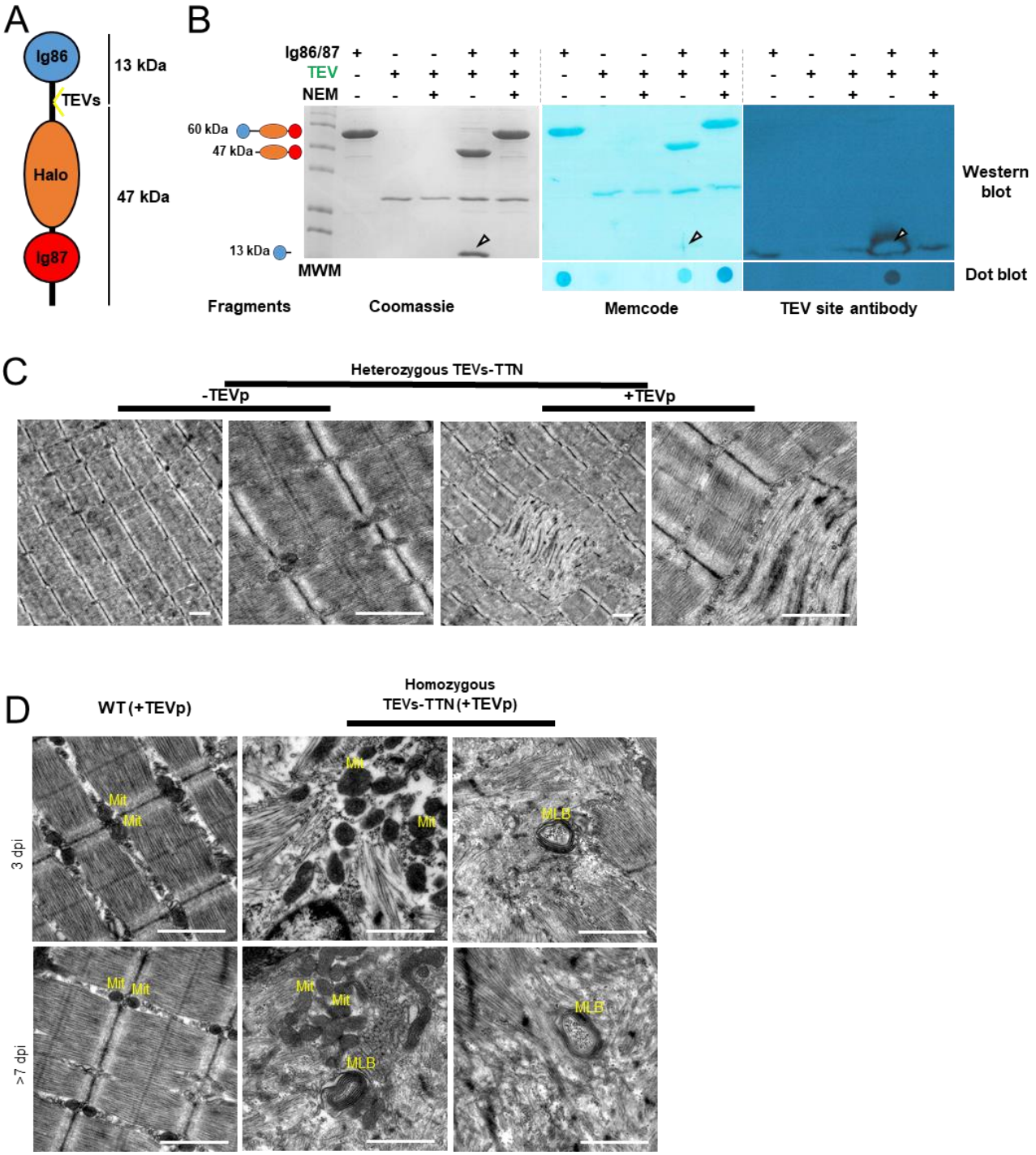

Figure S5. Sarcomere disassembly in titin mKO muscles. (A) Scheme of the recombinant Ig86-TEVs-Halo-Ig87 titin fragment that, upon TEV protease treatment, results in 13 kDa and 47 kDa fragments. **(B)** Validation of the specificity of anti-cTEVsite antibody by SDS-PAGE and WB (denaturing conditions) and dot-blot (native conditions). Ig86-TEVs-Halo-Ig87 is incubated with TEV protease to induce cleavage. A control sample where TEV protease activity is blocked by treatment with N-ethylmaleimide (NEM) is also included. Anti cTEVsite signal only occurs in samples where the 13-KDa fragment is present, both in native and denaturing conditions. Molecular weight marker (MWM) used in Coomassie was Precision Plus Protein Dual Color Standards (1610374, BioRad). **(C)** Transmission electron microscopy on longitudinal EDL sections of heterozygous muscles at different magnifications (representative images from n=2-4 animals). Scale bars represent 1 µm. **(D)** Transmission electron microscopy on longitudinal homozygous EDL sections of AAV6-injected WT and TEVs-TTN muscles (representative images from n=2-4 animals, Mit: Mitochondria, MLB: multilamellar body). Scale bars represent 1 µm.

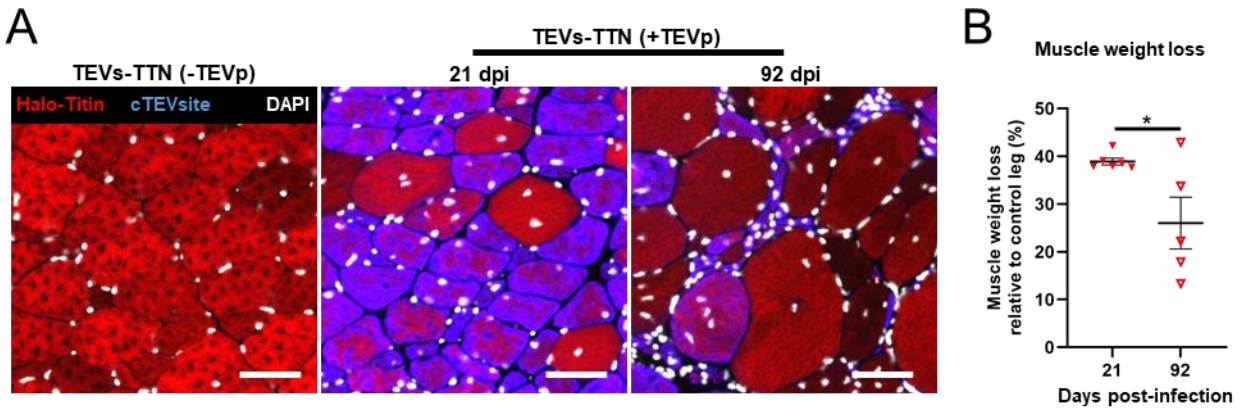

Figure S6. Titin mKO muscles at long time points. (A) Halo-Titin and cTEVsite immunofluorescence in AAV6-injected TEVs-TTN muscles at 21 and 92 dpi showing titin expression in myofibers that are cTEVsite-negative and have centrally-located myonuclei (representative images from n=4-5 animals). Scale bars represent 50 µm. **(B)** Muscle weight loss in AAV6-injected TEVs-TTN muscles relative to their contralateral control legs at 21 and 92 dpi (n=5-6). Part of these data are presented also in **Figure 1L.** Data are represented as mean ± SEM.

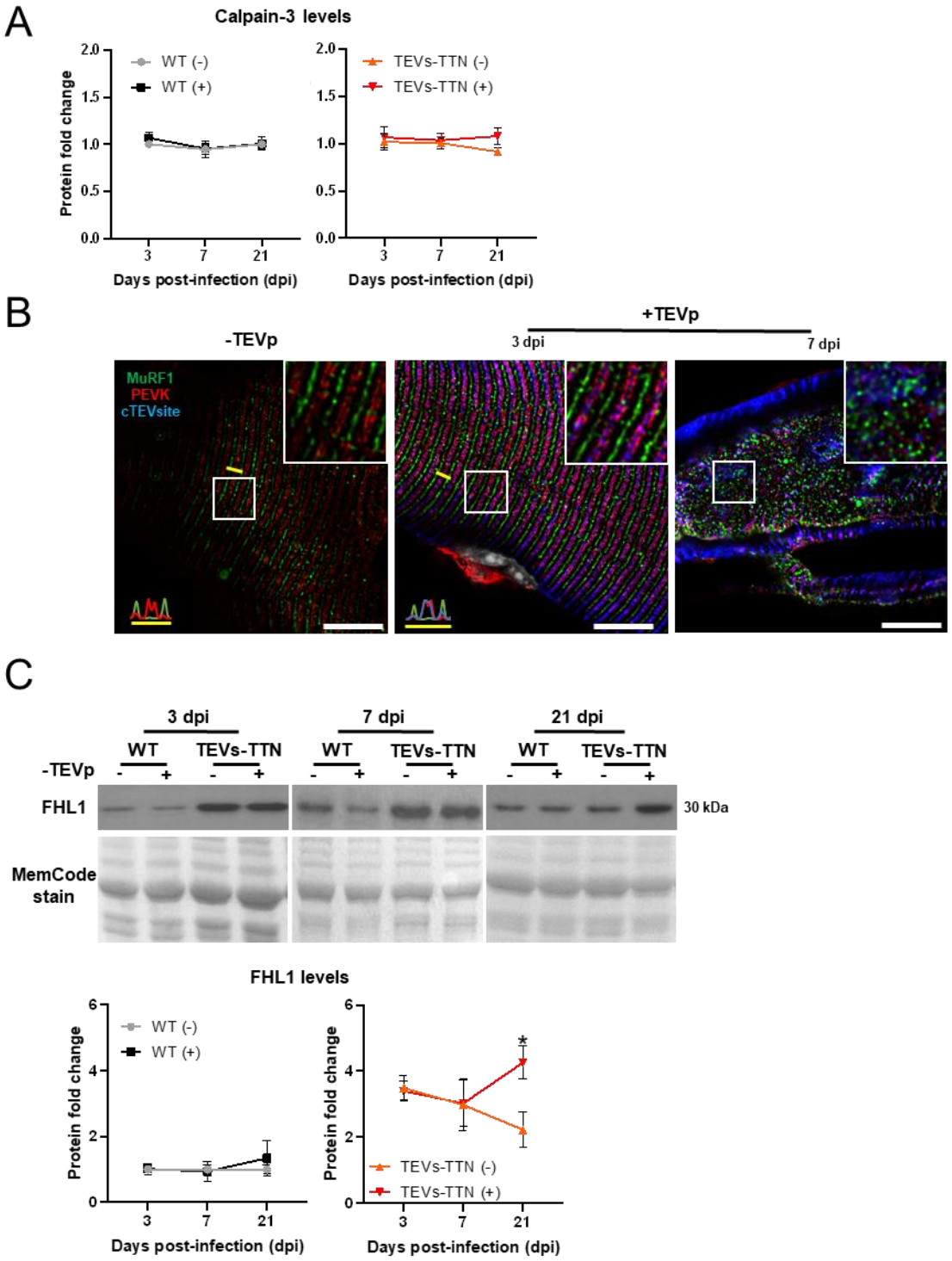

Figure S7. Localization and levels of titin-related proteins. (A) Total calpain 3 levels including cleaved and intact calpain 3 at the different timepoints as measured in western blot (n = 3-6 animals per condition). **(B)** FHL1 expression of the different titin interactors evaluated by WB (n=3-6). Memcode protein staining was used for normalization. Protein fold changes were calculated relative to WT NaCl-injected samples. Scale bars represent 10 µm. **(C)** MuRF1 immunofluorescence in control and AAV6-injected TEVs-TTN muscles at 3 and 7 dpi showing sarcomeric localization of the protein at 3 dpi and dotty staining in the absence of sarcomeres (as marked by antibodies against titin PEVK and cTEV site) at 7 dpi (representative images from n=3 animals). Normalized fluorescence intensity profile along the lines indicated in yellow are shown (for simplicity, the cTEVsite profile is not shown in the -TEVp sample). Data are represented as mean ± SEM.

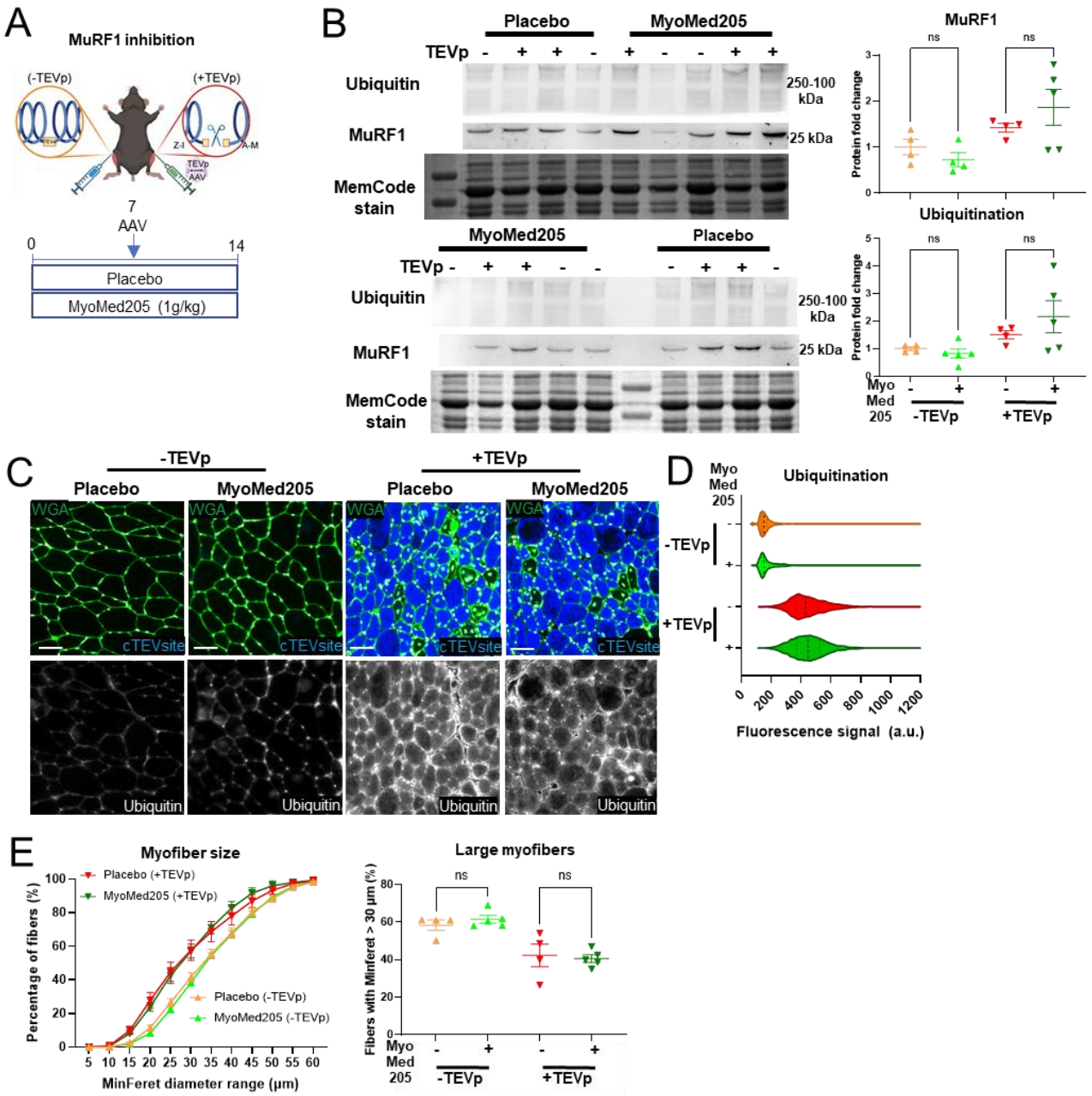

Figure S8. MyoMed205 treatment. (A) Homozygous TEVs-TTN mice were treated with MyoMed205 (1 g/kg) spiked food or control placebo diet for two weeks. Mice were intramuscularly injected with either saline solution or AAV6-GFP-TEVp at the first week of treatment and muscles were harvested 7 dpi. **(B)** MuRF1 and protein ubiquitination levels measured by WB (n= 4-5 animals). MemCode total protein staining was used for normalization. Protein fold changes were calculated relative to placebo-treated, NaCl-injected samples. **(C)** Representative cTEVsite and ubiquitin immunofluorescences. Scale bars represent 50 µm. **(D)** Violin plot quantification of intramyofiber ubiquitin fluorescence intensity (4100-7100 myofibers from n = 4-5 animals). **(E)** Analysis of myobofier size (n=4-5 animals). Data are represented as mean ± SEM.

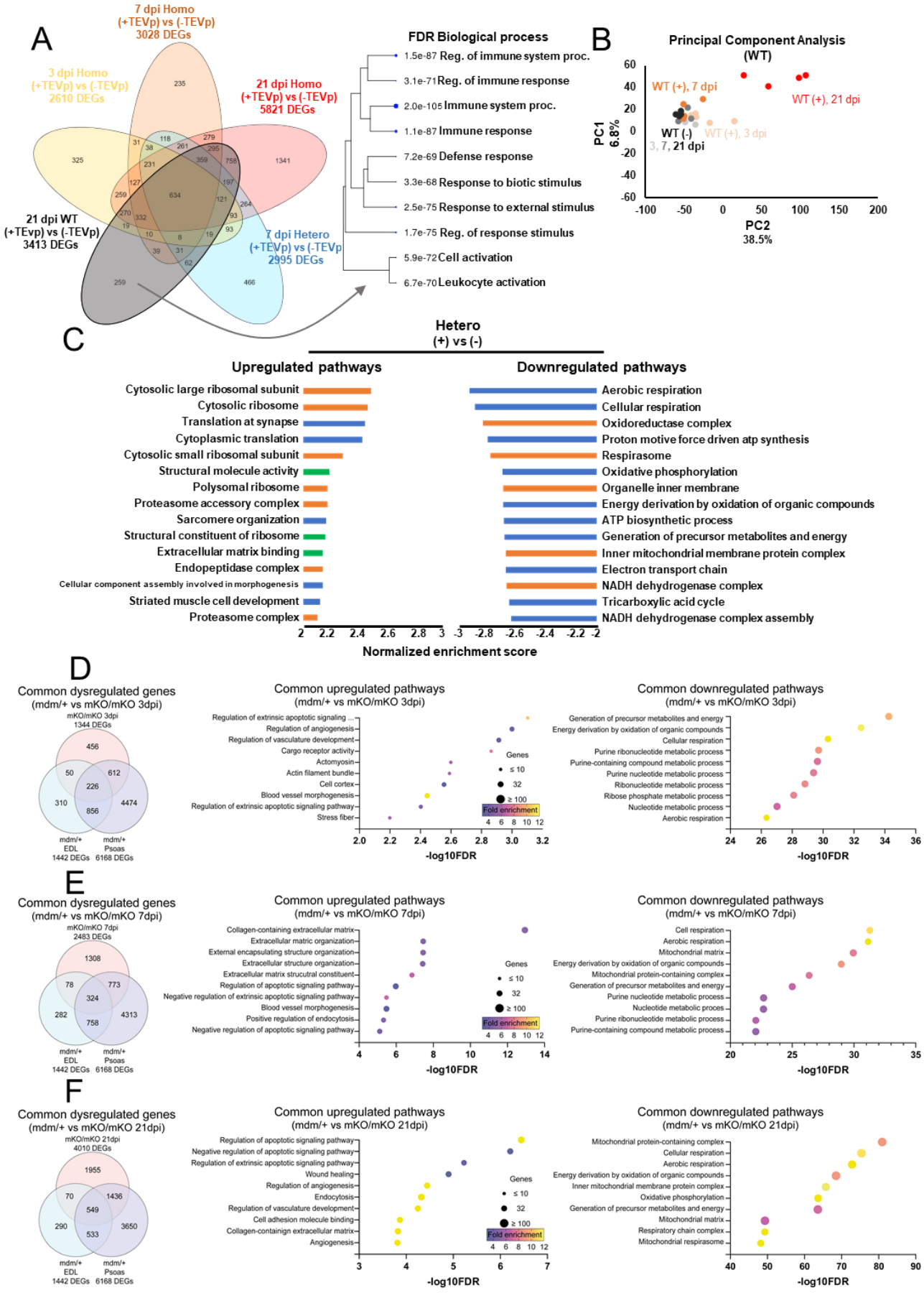
A
7 dpi Homo (+TEVp) vs (-TEVp) 3028 DEGs
3 dpi Homo (+TEVp) vs (-TEVp) 2610 DEGs
21 dpi Homo (+TEVp) vs (-TEVp) 5821 DEGs
21 dpi WT (+TEVp) vs (-TEVp) 3413 DEGs
7 dpi Hetero (+TEVp) vs (-TEVp 2995 DEGs
FDR Biological process
1.5e-87 Reg. of immune system proc.
3.1e-71 Reg. of immune response
2.0e-105 Immune system proc.
1.1e-87 Immune response
7.2e-69 Defense response
3.3e-68 Response to biotic stimulus
2.5e-75 Response to external stimulus
1.7e-75 Reg. of response stimulus
5.9e-72 Cell activation
6.7e-70 Leukocyte activation
B
Principal Component Analysis (WT)
WT (+), 7 dpi
WT (+), 21 dpi
WT (-)
WT (+), 3 dpi
3, 7, 21 dpi
PC1 6.8%
PC2 38.5%
C
Hetero (+) vs (-)
Upregulated pathways
Cytosolic large ribosomal subunit
Cytosolic ribosome
Translation at synapse
Cytoplasmic translation
Cytosolic small ribosomal subunit
Structural molecule activity
Polysomal ribosome
Proteasome accessory complex
Sarcomere organization
Structural constituent of ribosome
Extracellular matrix binding
Endopeptidase complex
Cellular component assembly involved in morphogenesis
Striated muscle cell development
Proteasome complex
Downregulated pathways
Aerobic respiration
Cellular respiration
Oxidoreductase complex
Proton motive force driven atp synthesis
Respirasome
Oxidative phosphorylation
Organelle inner membrane
Energy derivation by oxidation of organic compounds
ATP biosynthetic process
Generation of precursor metabolites and energy
Inner mitochondrial membrane protein complex
Electron transport chain
NADH dehydrogenase complex
Tricarboxylic acid cycle
NADH dehydrogenase complex assembly
Normalized enrichment score
D
Common dysregulated genes (mdm/+ vs mKO/mKO 3dpi)
mKO/mKO 3dpi 1344 DEGs
mdm/+ EDL 1442 DEGs
mdm/+ Psoas 6168 DEGs
Common upregulated pathways (mdm/+ vs mKO/mKO 3dpi)
Regulation of extrinsic apoptotic signaling ...
Regulation of angiogenesis
Regulation of vasculature development
Cargo receptor activity
Actomyosin
Actin filament bundle
Cell cortex
Blood vessel morphogenesis
Regulation of extrinsic apoptotic signaling pathway
Stress fiber
Genes
Fold enrichment
-log10FDR
Common downregulated pathways (mdm/+ vs mKO/mKO 3dpi)
Generation of precursor metabolites and energy
Energy derivation by oxidation of organic compounds
Cellular respiration
Purine ribonucleotide metabolic process
Purine-containing compound metabolic process
Purine nucleotide metabolic process
Ribonucleotide metabolic process
Ribose phosphate metabolic process
Nucleotide metabolic process
Aerobic respiration
-log10FDR
E
Common dysregulated genes (mdm/+ vs mKO/mKO 7dpi)
mKO/mKO 7dpi 2483 DEGs
mdm/+ EDL 1442 DEGs
mdm/+ Psoas 6168 DEGs
Common upregulated pathways (mdm/+ vs mKO/mKO 7dpi)
Collagen-containing extracellular matrix
Extracellular matric organization
External encapsulating structure organization
Extracellular structure organization
Extracellular matrix strucutral constituent
Regulation of apoptotic signaling pathway
Negative regulation of extrinsic apoptotic signaling pathway
Blood vessel morphogenesis
Positive regulation of endocytosis
Negative regulation of apoptotic signaling pathway
Genes
Fold enrichment
-log10FDR
Common downregulated pathways (mdm/+ vs mKO/mKO 7dpi)
Cell respiration
Aerobic respiration
Mitochondrial matrix
Energy derivation by oxidation of organic compounds
Mitochondrial protein-containing complex
Generation of precursor metabolites and energy
Purine nucleotide metabolic process
Nucleotide metabolic proces
Purine ribonucleotide metabolic process
Purine-containing compound metabolic process
-log10FDR
F
Common dysregulated genes (mdm/+ vs mKO/mKO 21dpi)
mKO/mKO 21dpi 4010 DEGs
mdm/+ EDL 1442 DEGs
mdm/+ Psoas 6168 DEGs
Common upregulated pathways (mdm/+ vs mKO/mKO 21dpi)
Regulation of apoptotic signaling pathway
Negative regulation of apoptotic signaling pathway
Regulation of extrinsic apoptotic signaling pathway
Wound healing
Regulation of angiogenesis
Endocytosis
Regulation of vasculature development
Cell adhesion molecule binding
Collagen-containign extracellular matrix
Angiogenesis
Genes
Fold enrichment
-log10FDR
Common downregulated pathways (mdm/+ vs mKO/mKO 21dpi)
Mitochondrial protein-containing complex
Cellular respiration
Aerobic respiration
Energy derivation by oxidation of organic compounds
Inner mitochondrial membrane protein complex
Oxidative phosphorylation
Generation of precursor metabolites and energy
Mitochondrial matrix
Respiratory chain complex
Mitochondrial respirasome
-log10FDR

Figure S9. Gene expression in titin mKO muscles. (A) Shared DEGs between AAV6-injected and saline- injected legs for WT muscles at 21 dpi, heterozygous TEVs-TTN muscles at 7 dpi and homozygous TEVs-TTN muscles at 3, 7 and 21 dpi (n=4). To the right, hierarchical clustering tree of the shared 3,413 DEGs between WT and the rest of the groups (n=4). **(B)** Principal component analysis of gene expression in WT TA muscles. **(C)** Dysregulated pathways in heterozygous titin mKO muscles. **(D-F)** Left, shared DEGs in heterozygous *mdm* EDL and psoas muscles[45], and homozygous titin mKO TA muscles at 3 (D), 7 (E), 21 (F) dpi. Middle and right, top 10 most dysregulated gene ontology terms of the corresponding shared DEGs at the different experimental times.

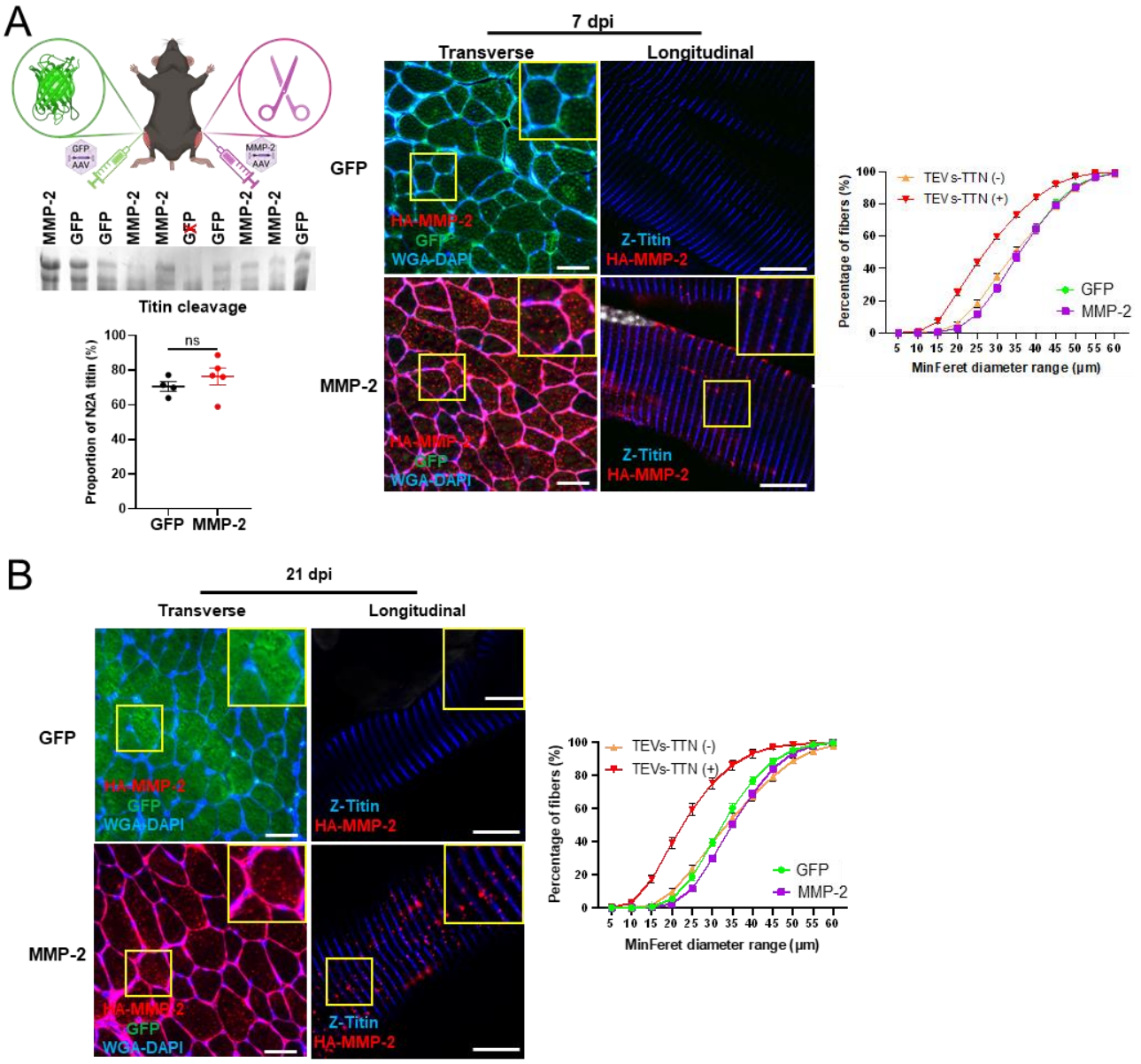

Figure S10. MMP-2 overexpression does not result in titin cleavage nor myopathic response. (A) Mice were intramuscularly injected with AAV6 vectors encoding either GFP or HA-tagged MMP-2. SDS-PAGE gel to stain titin did not show any effect on full length N2A titin at 7 dpi (n=4-5 animals, crossed sample was not analyzed due to technical titin degradation). Transverse TA sections evidence major HA-MMP-2 location in the interfiber space, but also intracellular dots. Longitudinal EDL sections evidence a location of HA-MMP-2 near the Z line of the sarcomeres without any sign of sarcomeric disarrays produced at 7 dpi. No effect was observed on myofiber size by the overexpression of MMP-2 (n=5 animals). Scale bars represent 50 µm for transverse sections and 10 for longitudinal sections. **(B)** The effect of MMP-2 overexpression was tested after 21dpi obtaining similar results in location and effects on myofiber size (n=-5-7 animals). Scale bars represent 50 µm for transverse sections and 10 for longitudinal sections. Data are represented as mean ± SEM. For reference, TEVs-TTN data from **Figure 2B** are also plotted in both panels

Table S1. GFP-uTEV3 expression by RNAseq (normalized counts).

	3 dpi (Mean ± SEM)	7 dpi (Mean ± SEM)	21 dpi (Mean ± SEM)
WT(-TEVp)	0.08 ± 0.05	0.03 ± 0.002	0.07 ± 0.04
WT (+TEVp)	17.17 ± 8.075	239.5 ± 34.14	756.1 ± 249.6
P value WT (-TEVp vs +TEVp)	0.036	0.0019	0.0286
TEVs-TTN(-TEVp)	0.143 ± 0.07	0.03 ± 0.001	0.09 ± 0.07
TEVs-TTN (+TEVp)	49.41 ± 10.9	22.41 ± 2.41	640.4 ± 215.7
P value TEVs-TTN (-TEVp vs +TEVp)	0.004	<0.0001	0.0286

Table S2. Antibodies used for western blot and immunofluorescence.

Experiment	Target	Host	Reference	Dilution	RRID
Western Blot	GFP	Rabbit	Abcam: Ab290	1:2000	AB_303395
Western Blot	Cleaved TEVsite (cTEVsite)	Rabbit	Novus Bio: NBP2-37831	1:1000	AB_3297347
Western Blot	ANKRD1	Rabbit	MYOMEDIX: Ankrd1-1	1:1000	
Western Blot	Calpain-3	Rabbit	MYOMEDIX: CAPN3	1:1000	
Western Blot	FHL1	Rabbit	Aviva: ARP34378_T100	1:1000	AB_842144
Western Blot	HSP27	Mouse	DSHB: CPTC-HSPB1-1	1:250	AB_2617268
Western Blot	αβ-crystallin	Mouse	DSHB CPTC-CRYAB-2	1/250	AB_1553792
Western Blot	MuRF1	Chicken	MYOMEDIX MuRF1-3	1/1000	
Western Blot	Ubiquitin	Mouse	Santa Cruz: sc-8017	1:250	AB_628423
Western Blot	Rabbit IgG (Peroxidase-coupled antibody)	Goat	Sigma: A0545-1mL	1/5000	AB_257896
Western Blot	Mouse IgG	Goat	Thermo: 31430	1:5000	AB_228307

	(Peroxidase-coupled antibody)				
Western Blot	Chicken IgY (Peroxidase-coupled antibody)	Goat	Thermo: A16054	1:5000	AB_2534727
Immunofluorescence	GFP	Chicken	Thermo: A10262	1:100	AB_2534023
Immunofluorescence	Desmin	Rabbit	Abcam: Ab15200	1:200	AB_301744
Immunofluorescence	Cleaved TEVsite (cTEVsite)	Rabbit	Novus Bio: NBP2-37831	1:100	AB_3297347
Immunofluorescence	PEVK-Titin	Mouse (IgM)	DSHB: D910	1:10	
Immunofluorescence	α-actinin	Mouse	Sigma: A7732	1:100	AB_2221571
Immunofluorescence	Ubiquitin	Mouse	Santa Cruz: sc-8017	1:50	AB_628423
Immunofluorescence	Z-Titin	Mouse	Homemade: T12	1:20	
Immunofluorescence	MuRF1	Chicken	MYOMEDIX: MuRF1-3	1:100	
Immunofluorescence	HA tag (MMP-2 immunofluorescence)	Goat	Cell Signaling: 3724S	1:500	AB_1549585
Immunofluorescence	Chicken IgY (Alexa 488-coupled antibody)	Goat	Thermo: A-11039	1:500	AB_2534096
Immunofluorescence	Rabbit IgG (Alexa 647-coupled antibody)	Goat	Thermo: A-21245	1:500	AB_2535813
Immunofluorescence	Rabbit IgG (Alexa 488-coupled antibody)	Goat	Thermo: A-11034	1:500	AB_2576217
Immunofluorescence	Mouse IgM (Alexa 546-coupled antibody)	Goat	Thermo: A-21045	1:500	AB_2535714
Immunofluorescence	Mouse IgG (Alexa 647-coupled antibody)	Chicken	Thermo: A-21463	1:500	AB_2535869
Immunofluorescence	Mouse IgG (Alexa 568-coupled antibody)	Goat	Thermo: A-11031	1:500	AB_144696
Immunofluorescence	Rabbit IgG	Goat	Thermo: A-32732	1:500	AB_2633281

(Alexa 555-coupled antibody)